XLVI CILAMCE
VITÓRIA - ES - BRAZIL - 2025
XLVI IBERO-LATIN AMERICAN CONGRESS ON COMPUTATIONAL METHODS IN ENGINEERING

A simple mass-conserved Level Set Method for FSI problems with free-surface flows

Mateus Guimarães Tonin[1], Alexandre Luis Braun[2]

[1]*Universidade Federal da Fronteira Sul*
ERS-135, km 72, nº 200, 99700-970, Erechim - RS, Brazil
mateus.tonin@uffs.edu.br
[2]*Programa de Pós-Graduação em Engenharia Civil, Universidade Federal do Rio Grande do Sul*
Av. Osvaldo Aranha 99, 90035-190, Porto Alegre - RS, Brazil
alexandre.braun@ufrgs.br

Abstract. In the present work, numerical simulations of Fluid-Structure Interaction (FSI) problems are carried, involving floating bodies subjected to the action of free-surface flows. The free-surface treatment is considered using the Level Set Method (LSM), which historically has a drawback of being too dissipative, leading to mass conservation errors. In a relatively new modification, proposed by Yuan et al. [1] and implemented here, a source or sink term is introduced into the original level set equation to compensate the mass loss or offset the mass increase, leading to better results. Also, in our model the fluid equations are discretized using the Characteristic-Based Split (CBS) method in the context of the Finite Element Method (FEM). The structure is kinematically described using a rigid body approach. The system of equations of motion is discretized in time using the implicit Newmark and α-Generalized methods. Several problems are simulated, comparing the results with those from the original level set method, demonstrating that the modified version has the capability of accurately capture the interface and keep the mass conservation.

Keywords: Level Set Method; Floating Structures; Fluid-Structure Interaction; Free-Surface Flows.

1 Introduction

One of the major difficulties involving a floating body simulation is relative to the tracking of the free-surface. In this regard, many interface tracking methods have been developed (see, for example Cruchaga et al. [2]), being the LSM, proposed by Osher and Sethian [3], one of the most popular methods due to its easiness of implementation and in capturing interfaces changes (like breakups or coalescences), and also because it can accurately calculate geometric properties, like the curvature, for example. Unfortunately, the LSM is notorious for being a dissipative method, leading to mass losses, especially in regions involving high curvatures (Jiang et al. [4]). More recently, Yuan et al. [1] proposed a simple modification of the original LSM, where a source or sink term is introduced in the Level Set equation to compensate the mass loss or offset the mass increase, leading to better results relative to the original method.

In the present work, the flow equations are discretized using the CBS method considering a semi-implicit scheme. For the turbulence treatment, it's employed the Large Eddy Simulation (LES) methodology, using the classical and dynamic Smagorinsky models for scales below mesh resolution. For the spatial discretization, the FEM is employed using linear tetrahedral elements. As mentioned before, the LSM is used for the treatment of the free surface flows, considering the modifications proposed by Yuan et al. [1]. For the analysis of flows in the presence of moving bodies, an Arbitrary Lagrangian-Eulerian (ALE) formulation is used to describe the movement of fluid particles, with a mesh movement scheme employed previously by Braun [5]. The solid body is treated using a rigid body approach. The temporal discretization is performed using the implicit Newmark and α-Generalized methods. For the analysis of FSI problems, an explicit partitioned model is used.

2 Formulation

2.1 Flow analysis

In the present model, the flow is considered incompressible, consisting of a Newtonian fluid in an isothermal condition and without mass or energy transport. Therefore, essentially the Navier-Stokes equations and the mass balance are used.

The Navier-Stokes equations, expressed in orthogonal Cartesian coordinates and in an arbitrary Lagrangian-Eulerian (ALE) kinematic description, are given by:

$$\frac{\partial v_i}{\partial t} + \left(v_j - w_j\right)\frac{\partial v_i}{\partial x_j} = g_i - \frac{1}{\rho_f}\frac{\partial p}{\partial x_i} + \nu\frac{\partial^2 v_i}{\partial x_j^2} \qquad (i,j,k = 1,2,3), \tag{1}$$

where ρ_f is the specific mass of the fluid, v_i the components of the flow velocity vector **v**, w_i the components of the mesh velocity vector **w**, t the time, x_i the components of the position vector **x** along the coordinate axes, g_i the components of the acceleration vector of gravity **g**, p the thermodynamic pressure, δ_{ij} the Kronecker delta components and ν the kinematic viscosity coefficient.

The mass conservation equation can be expressed (considering an incompressible fluid) by the equation:

$$\frac{\partial v_i}{\partial x_i} = 0 \qquad (i = 1,2,3). \tag{2}$$

2.2 Free surface

For the free-surface flows, the LSM is adopted, where a scalar distance function with sign ϕ is used, in such a way that the separation interface between fluids is located at the positions where $\phi = 0$. The total area Ω is filled by a liquid region (where $\phi > 0$ was defined) and several gaseous regions ($\phi < 0$); with the interface ($\phi = 0$) represented by the lines Γ_F (see Sussman et al. [6]). The equation that describes the evolution of the ϕ function over time is given by (Sussman et al. [6]):

$$\frac{\partial \phi}{\partial t} + v_j\frac{\partial \phi}{\partial x_j} = 0 \qquad \left(j = 1,2,3\right). \tag{3}$$

The fluid physical properties are then defined as functions of ϕ, as shown in eq. (4). ρ_1 and ρ_2 are the fluid specific masses corresponding to fluids 1 and 2, respectively, and $H(\phi)$ is a "smoothed" Heaviside function. ε is the half-thickness of the transition zone, normally defined as $\varepsilon = \alpha_{LS}.\Delta x$, where Δx is the characteristic dimension of an element at the interface region and α_{LS} is a model parameter with values varying between 1 and 2.

$$\rho(\phi) = \rho_1 + (\rho_2 - \rho_1)H(\phi), \text{ being } H(\phi) = \begin{cases} 0 & \text{for } \phi < -\varepsilon \\ \frac{1}{2}\left[1 + \frac{\phi}{\varepsilon} + \frac{1}{\pi}\sin\left(\frac{\pi\phi}{\varepsilon}\right)\right] & \text{for } |\phi| \le \varepsilon \\ 1 & \text{for } \phi > \varepsilon \end{cases}. \tag{4}$$

The numerical solution of eq. (3) does not guarantee that ϕ will remain as a distance function (i.e. $|\nabla\phi| = 1$), thus a reinitialization procedure is necessary to ensure this condition (see Sussman et al. [7]).

Unfortunately, the LSM suffers greatly from mass losses. To solve this issue, a modification proposed by Yuan et al. [1] is implemented here, where a source or sink term $q(x,t)$ is added into eq. (3) in order to offset the effect of numerical diffusion on non-conservation of mass:

$$\frac{\partial \phi}{\partial t} + v_j\frac{\partial \phi}{\partial x_j} = q\left(x,t\right) \qquad \left(j = 1,2,3\right). \tag{5}$$

As the numerical diffusion is very small at each time step, it can be assumed that the distribution of the source is uniform in the whole domain, and then $q(t)$ is only a function of time (Yuan et al.[1]), being defined as:

$$q(t) = \frac{\sum_{\Omega} \rho H(\phi) - M_0}{\Delta t \sum_{\Omega} \rho \delta(\phi)}, \tag{6}$$

being δ the Dirac delta function, which, like the Heaviside function, may be smoothed as follows:

$$\delta(\phi) = \frac{dH(\phi)}{d\phi} = \begin{cases} \frac{1}{2}\left[1 + \frac{\phi}{\varepsilon} + \frac{1}{\pi}\sin\left(\frac{\pi\phi}{\varepsilon}\right)\right] & \text{for} \quad |\phi| < \varepsilon \\ 0 \quad \text{for} \quad |\phi| \geq \varepsilon \end{cases}. \tag{7}$$

Finally, Δt is the time step, and M_0 the total mass of fluid phase satisfying $\phi < 0$ at $t = 0$.

2.3 Rigid Body Dynamics and FSI Modeling

The structure is idealized as a rigid body, considering that the displacements and rotations generated by the flow are much greater than the body deformations. The dynamic equilibrium equation is given by:

$$\mathbf{M}_S \ddot{\mathbf{U}}_S^c + \mathbf{C}_S \dot{\mathbf{U}}_S^c + \mathbf{K}_S \mathbf{U}_S^c = \mathbf{Q}_S^c, \tag{8}$$

where $\mathbf{M}_S$ is the mass matrix, $\mathbf{C}_S$ is the damping matrix, $\mathbf{K}_S$ is the stiffness matrix and $\mathbf{U}_S^c$, $\dot{\mathbf{U}}_S^c$ and $\ddot{\mathbf{U}}_S^c$ are the generalized displacement, velocity and acceleration vectors, respectively; while $\mathbf{Q}_S^c$ is the force vector. The subscript S is related to the structure, and the superscript c is related to the center of gravity of the structure.

A partitioned scheme is utilized here for the FSI coupling, where the flow and structural domains are solved sequentially by imposing kinematic compatibility and equilibrium conditions at the fluid-structure interface (see Braun [5].

3 Applications

3.1 Reyleigh-Taylor Instability

In this problem, a layer of a heavy fluid is situated above a lighter layer of fluid in the presence of a gravitational field. From this, a given disturbance is performed at the interface between the two fluids and the buoyancy forces will make this disturbance increase with time. Figure 1 shows more details, and also the mesh employed, which consists of 395,000 tetrahedral elements and 159,192 nodes, distributed non-uniformly.

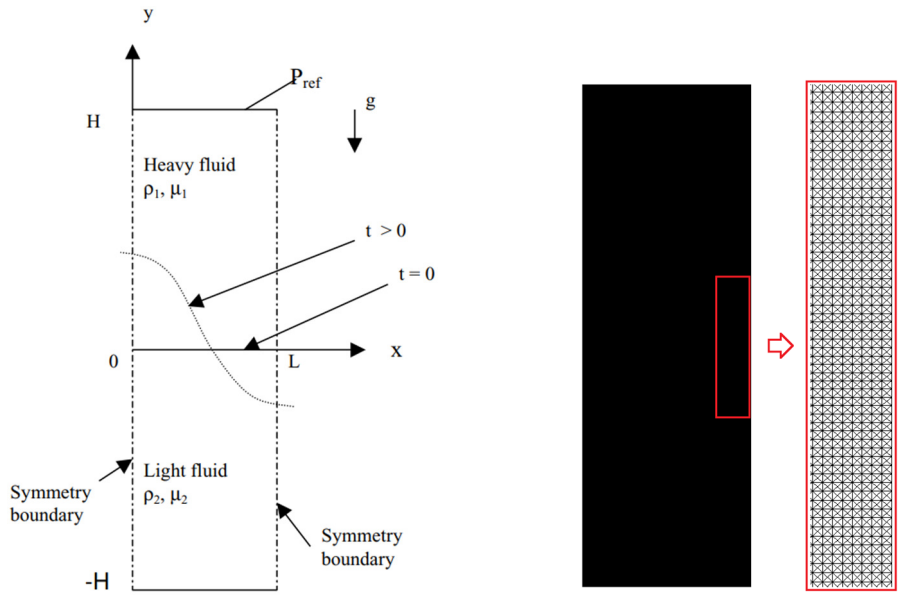


Figure 1. Rayleigh-Taylor Instability (left) (Zhao et al. [8]); and mesh adopted (right).

The height of the domain is $2H$ and the width is L. A boundary condition of symmetry is imposed on the sides and a wall is placed on the upper and lower edges. The ratio between specific masses of fluids (ρ_1/ρ_2) is equal to two and both fluids have the same kinematic viscosities. This problem has been studied by several authors, including the numerical studies by Zhao et al. [8] and Kelecy and Pletcher [9]. The Reynolds number studied in this work is 283. The perturbation equation is given in the form:

$$\frac{u}{U_{ref}} = \begin{cases} \alpha \sin\left(\frac{\pi x}{L}\right) \exp\left(-\frac{\pi |y|}{L}\right), & \frac{y}{L} > 0 \\ -\alpha \sin\left(\frac{\pi x}{L}\right) \exp\left(-\frac{\pi |y|}{L}\right), & \frac{y}{L} < 0 \end{cases}, \tag{9}$$

$$\frac{v}{U_{ref}} = \alpha \cos\left(\frac{\pi x}{L}\right) \exp\left(-\frac{\pi |y|}{L}\right). \tag{10}$$

In Zhao et al. [8], α is defined as 0.25, which is also adopted here.

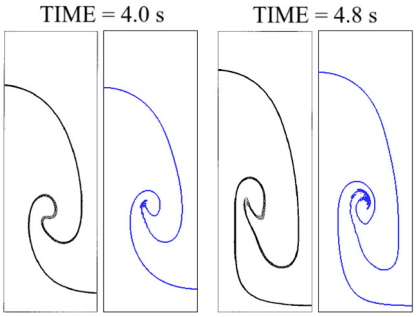


Figure 2. Interface movement for the Rayleigh-Taylor instability: comparison between the results of Kelecy and Pletcher [9] (left); and the present work, using classic LSM (right).

Figure 2 shows the results of the interface movement obtained from the present work, using the classic LSM, being compared with the results presented by Kelecy and Pletcher [9], where it can be seen that both results agree quite well. Unfortunately, the classic LSM lost some volume during the process, around 1.2%, as shown in Figure 3 (left). Using the mass-conserved LSM, it can be seen that the volume is conserved pretty well. Finally, Figure 3 (right) shows a comparison of the last movement of the interface (at time 4.8 s) between the classic and modified LSM, showing that the modified LSM also improves the quality of the interface.

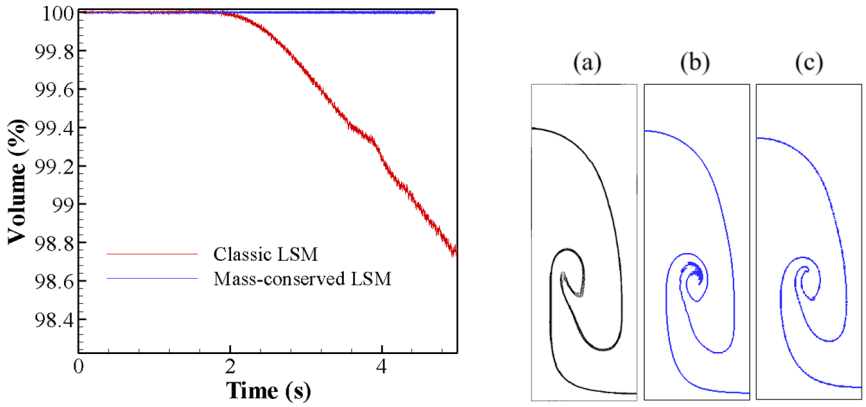


Figure 3. Volume comparison between classic and mass-conserved LSM (left); and comparison of interfaces between: (a) Kelecy and Pletcher [9], (b) Classic LSM, and (c) Mass-conserved LSM at time 4.8 s (right).

3.2 Broken Dam Problem

The present example is utilized to verify the numerical model proposed in this work when flow problems with free surfaces are considered. This application was studied first by Martin and Moyce [10] using experimental techniques. In this problem, a column of water falls over a flat horizontal surface. Figure 4 shows a schematic view of the problem, along with the mesh proposed in this study.

The size of the computational domain employed here is defined as $5a \times 1.25a \times a$, being $a = 0.0571504$ m, along the x, y and z directions, respectively. The mesh used consists in 1,377,120 tetrahedral elements, distributed in a non-uniform way. The boundary conditions used are a no slip wall at the bottom surface and free-slip walls at the others surfaces. The smallest element, located next to the walls, has a length of 3.94×10^{-4} m. Figure 5 shows results obtained here, using the classic LSM and the mass-conserved version, referring to the surge s and remaining height h, which are compared with predictions obtained experimentally by Martin and Moyce [10] and numerically by Lin et al. [11]. Notice that a dimensionless time $t_g = (a/g)^{0.5}$ is adopted for both graphics.

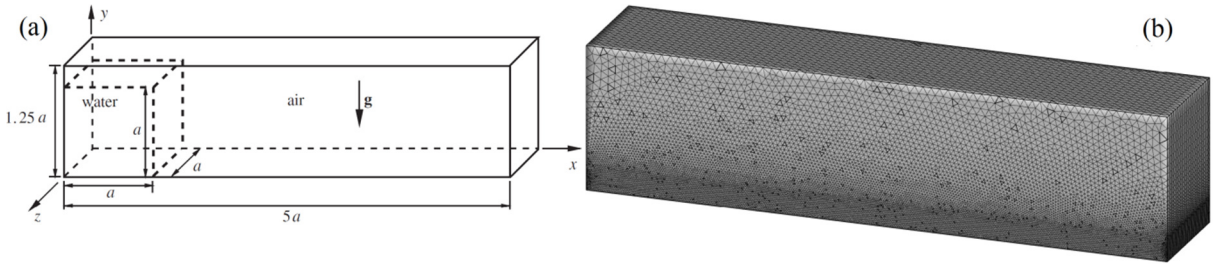


Figure 4. (a) Schematic view of the 3D broken dam problem (Lin et al. [11]); and (b) Mesh proposed by the study.

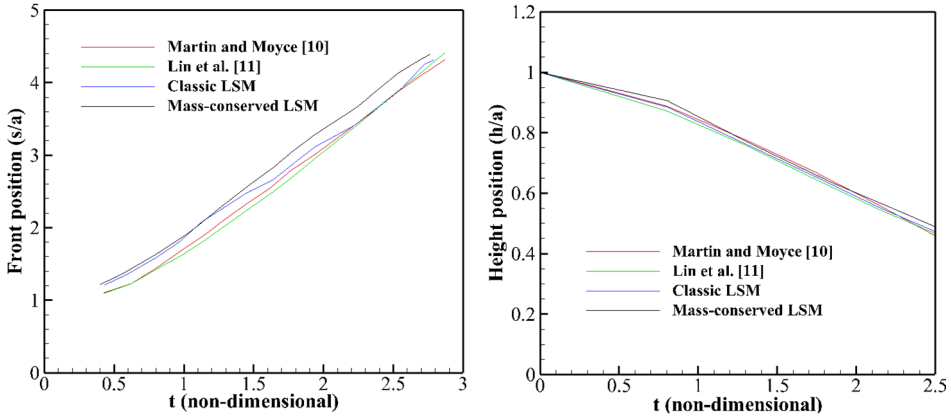


Figure 5. Surge (left) and remaining height (right) for the broken dam problem.

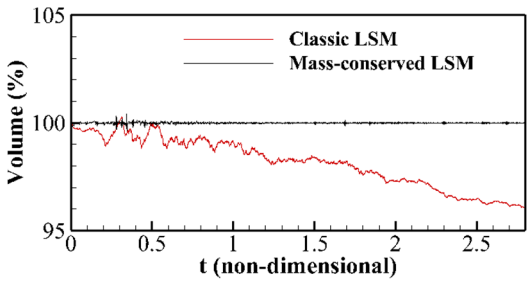


Figure 6. Volume comparison between classic and mass-conserved LSM.

One can see that a good agreement is obtained with respect to the references results, especially when the

water column height h is considered. Comparing the two LSM proposed, it can be noticed from the surge results that the mass-conserved scheme is less dissipative, conserving better not only the mass, but the energy of the system as well. Figure 6 compares the conservation of volume between the two schemes, showing again that the source or sink term improves the mass conservation.

At last, the evolution of the free surface over time is shown in Figure 7 for some dimensionless time instants, where it is observed that the physical aspects of the flow are reproduced accurately.

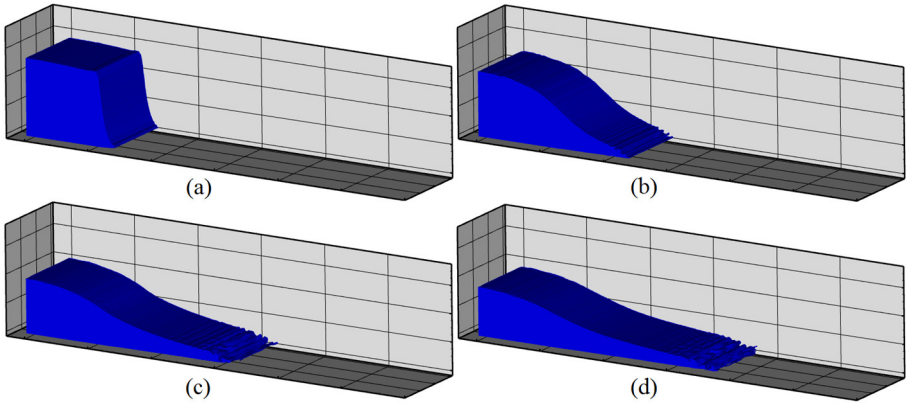


Figure 7. Free surface configurations for some dimensionless time instants: (a) t = 0.432; (b) t = 1.129; (c) t = 1.641; (d) t = 1.941.

3.3 Transient heave oscillation of a floating cylinder

The oscillation of a buoyant body on the water surface is investigated in this last application. This problem was proposed by Zandbergen et al. [12], and later studied by Donescu and Virgin [13] and Sanders et al. [14]. A circular cylinder is considered in a tank of water, with density equal to half of the water density, so that the equilibrium position corresponds to a configuration where the body is approximately half submerged. The circular cylinder presents a 2 m radius, which is released from an initial position (0.5 m above the water surface) in the middle of a tank with 100 m length and 4 m depth. Free-slip conditions are imposed as boundary conditions for all the surfaces of the domain and also zero pressure at the top surface. The physical properties utilized in the present simulations are defined as follows: for the liquid phase, $\rho = 10^3$ kg/m³ is the water specific mass and $\mu = 10^{-3}$ kg/m.s is the water viscosity; for the gaseous phase, $\rho = 1$ kg/m³ is the air density and $\mu = 2\text{x}10^{-5}$ kg/m.s is the air viscosity.



Figure 8. Mesh adopted.

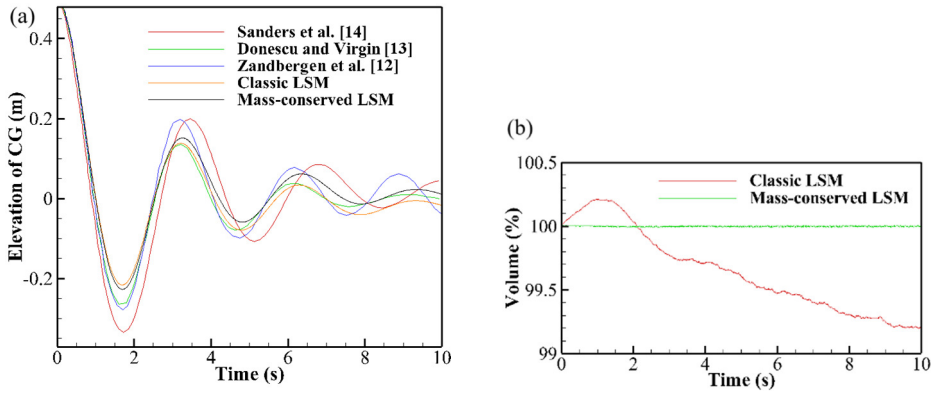


Figure 9. (a) Heave decay results for the buoyant cylinder problem; (b) Volume comparison between classic and mass-conserved LSM.

The mesh used consists in 406,317 tetrahedral elements, distributed in a non-uniform way, as shown in Figure 8. The smallest element length Δx is 0.0264 m, which is located next to the fluid-structure interface and around the free surface. As for the results, from Figure 9 (a), one can see that predictions obtained with the two LSM schemes proposed here agree well with the numerical results presented by Donescu and Virgin [13]; and the mass-conserved scheme gives better results, probably due to the smaller dissipation presented, which helped to better conserve the energy of the fluid-structure system. Finally, Figure 9 (b) shows the comparison of volumes between the two schemes, showing again the better mass conservation properties of the new scheme.

4 Conclusions

From the results, it is observed that the newly implemented source or sink term in the LSM is able to better conserve the original volume (or mass) of the simulations. This, in turn, also helped to improve the quality of the free surface interface, especially in regions with high curvatures. Last but not least, the new term also helped to better preserve the energies of the fluids, which, in turn, improved the energy transfer that occurs at the fluid-structure interfaces, leading to better results.

Acknowledgements. The authors would like to thank CNPq and CAPES for their financial support to this ongoing research. The research was developed with the support of the Núcleo Avançado de Computação de Alto Desempenho (NACAD) at COPPE, at Universidade Federal do Rio de Janeiro (UFRJ); the Centro Nacional de Processamento de Alto Desempenho em São Paulo (CENAPAD-SP); and the Laboratório Nacional de Computação Científica (LNCC).

Authorship statement. The authors hereby confirm that they are the sole liable persons responsible for the authorship of this work, and that all material that has been herein included as part of the present paper is either the property (and authorship) of the authors, or has the permission of the owners to be included here.

References

[1] H. -Z. Yuan, C. Shu, Y. Wang and S. Shu, "A simple mass-conserved level set method for simulation of multiphase flows". *Physics of Fluids*, vol. 30, pp. 1–14, 2018.
[2] M. Cruchaga, L. Battaglia, M. Storti and J. D'Elía. "Numerical modeling and experimental validation of free surface flow problems". *Archives of Computational Methods in Engineering*, vol. 23, pp. 139-169, 2016.
[3] S. Osher and J. Sethian. "Fronts propagating with curvature-dependent speed-algorithms based on Hamilton-Jacobi formulations". *Journal of Computational Physics*, vol. 79, pp. 12–49, 1988.
[4] L. Jiang, F. Liu and D. Chen. "A fast particle level set method with optimized particle correction procedure for interface capturing". *Journal of Computational Physics*, vol. 299, pp. 804–819, 2015.
[5] A. L. Braun. *Um modelo para simulação numérica da ação do vento sobre seções de ponte*. Masters dissertation, Universidade Federal do Rio Grande do Sul, 2002.
[6] M. Sussman, A. S. Almgren, J. B. Bell, P. Colella, L. H. Howell and M. L. Welcome, "An adaptive Level Set approach for incompressible two-phase flows". *Journal of Computational Physics*, vol. 148, pp. 81–124, 1999.
[7] M. Sussman, P. Smereka and S. Osher, "A level set approach for computing solutions to incompressible two-phase flow". *Journal of Computational Physics*, vol. 114, pp. 146–159, 1994.
[8] Y. Zhao, H. H. Tan, B. Zhang. "A high-resolution characteristics-based implicit dual time-stepping VOF method for free surface flow simulation on unstructured grids". *Journal of Computational Physics*, vol. 183, pp. 233–273, 2002.
[9] F. J. Kelecy, R. H. Pletcher. "The development of a free surface capturing approach for multidimensional free surface flows in closed containers". *Journal of Computational Physics*, vol. 138, pp. 939–980, 1997.
[10] J. C. Martin and W. J. Moyce. "An experimental study of the collapse of liquid columns on a rigid horizontal plate". *Philosophical Transactions of The Royal Society of London Series A*, vol. 244, pp 312 – 324, 1952.
[11] C. Lin, H. Lee, T. Lee and L. Weber. "A level set characteristic Galerkin finite element method for free surface flows". *International Journal for Numerical Methods in Fluids*, vol. 49, pp. 521 – 547, 2005.
[12] P. J. Zandbergen, J. Broeze, E. F. G. Van Daalen. "A panel method for the simulation of nonlinear gravity waves and ship motions". In: J. H. Kane, G. Maier, N. Tosaka, S. N. Atluri (ed.), *Advances in Boundary Element Techniques*. Springer: Berlin, 1993, pp. 486–509.
[13] P. Donescu and L. N. Virgin. "An implicit boundary element solution with consistent linearization for free surface flows and non-linear fluid-structure interaction of floating bodies". *International Journal for Numerical Methods in Engineering*, vol. 51, pp. 379–412, 2001.
[14] J. Sanders, J. E. Dolbow, P. J. Mucha and T. A. Laursen. "A new method for simulating rigid body motion in incompressible two-phase flow". *International Journal For Numerical Methods in Fluids*, vol. 67, n. 6, pp. 713–732, 2011.